Enrichment of submicron sea salt-containing particles in small cloud droplets based on single particle mass spectrometry

Qinhao Lin[1], Yuxiang Yang[1,2], Yuzhen Fu[1,2], Guohua Zhang[1], Feng Jiang[1,2], Long Peng[1,2], Xiufeng Lian[1,2], Fengxian Liu[1,2,#], Xinhui Bi[1,*], Lei Li[3], Duohong Chen[4], Mei Li[3], Jie Ou[5], Mingjin Tang[1], Xinming Wang[1], Ping'an Peng[1], and Guoying Sheng[1]

[1] State Key Laboratory of Organic Geochemistry and Guangdong Key Laboratory of Environmental Resources Utilization and Protection, Guangzhou Institute of Geochemistry, Chinese Academy of Sciences, Guangzhou 510640, PR China

[2] University of Chinese Academy of Sciences, Beijing 100039, PR China

[3] Institute of Mass Spectrometer and Atmospheric Environment, Jinan University, Guangzhou 510632, PR China

[4] State Environmental Protection Key Laboratory of Regional Air Quality Monitoring, Guangdong Environmental Monitoring Center, Guangzhou 510308, PR China

[5] Shaoguan Environmental Monitoring Center, Shaoguan 512026, PR China

[#] Present at College of Economics and Management, Taiyuan University of Technology, Taiyuan 030024, PR China

*Correspondence to: Xinhui Bi (bixh@gig.ac.cn)

Abstract. The effects of chemical composition and size of sea salt-containing particles on their cloud condensation nuclei (CCN) activity are incompletely understood. We used a ground-based counterflow virtual impactor (GCVI) coupled with a single particle aerosol mass spectrometer (SPAMS) to characterize chemical composition of submicron (dry diameter of 0.2-1.0 μm) and supermicron (1.0-2.0 μm) sea salt-containing cloud residues (dried cloud droplets) at Mount Nanling, southern China. Seven cut sizes (7.5-14 μm) of cloud droplets were set in the GCVI system. The highest number fraction of sea salt-containing particles was observed at the cut size of 7.5 μm (26%, by number), followed by 14 μm (17%), and the other cut sizes (3-5%). The submicron sea salt-containing cloud residues contributed approximately 20% (by number) at the cut size of 7.5 μm, which was significantly higher than the percentages at the cut sizes of 8-14 μm (below 2%). This difference was likely to be involved in the change of the chemical composition. At the cut size of 7.5 μm, nitrate was internally mixed with over 90% of the submicron sea salt-containing cloud residues, which was higher than sulfate (20%), ammonium (below 1%), amines (6%), hydrocarbon organic species (2%), and organic acids (4%). However, at the cut sizes of 8-14 μm, nitrate, sulfate, ammonium, amines, hydrocarbon organic species, and organic acids were internally mixed with > 90%, > 80%, 39-84%, 71-86%, 52-90%, and 32-77% of the submicron sea salt-containing cloud residues. The proportion of sea salt-containing particles in the supermicron cloud residues generally increased as a function of cut size, and their CCN activity was less influenced by chemical composition. This study

provided a significant contribution towards a comprehensive understanding of sea salt CCN activity.

1 Introduction

Atmospheric aerosol particles can directly influence the global radiative forces by scattering and absorbing solar radiation, and can indirectly influence them by serving as cloud condensation nuclei (CCN) (Boucher et al., 2013). The oceans represent one of the largest sources of natural aerosols with an estimated global production rate of 2000-10 000 Tg/yr (Gantt and Meskhidze, 2013). Modeling simulations showed that the indirect radiative forces of sea salt particles were about twice those of the direct forces (Ma et al., 2008). The addition of the sea salt particles over the remote ocean was estimated to enhance its CCN concentration by up to 500% (Pierce and Adams, 2006). The ability of sea salt particles acting as CCN is dependent on their size and chemical composition at a specific supersaturation (Andreae and Rosenfeld, 2008). Therefore, it is important to evaluate the impact of chemical composition and particle size on the CCN behavior of sea salt particles.

Numerous studies have revealed that fresh sea salt particles consist of inorganic salts and biologically produced organic species rather than just sodium chloride (NaCl) (Prather et al., 2013; Quinn et al., 2015; Bertram et al., 2018). The size-resolved chemical composition of fresh sea spray aerosols is dependent on complex factors including biological sources (e.g., phytoplankton and bacteria), physicochemical (e.g., sea surface active organic species) properties, and wind speeds (Quinn et al., 2015). Previous studies have shown that an increasing fraction of fresh sea salt particles is an internal mixture of inorganic salts (mainly including NaCl) and organic species as a result of the decreasing particle size (Prather et al., 2013; Bertram et al., 2018). However,

the fraction of organics (i.e., aliphatic organic material) in small sea spray aerosols exhibited some levels of variability in the similar simulation of ocean seawater conditions (Wang et al., 2015). Heterogeneous/multiphase reactions or atmospheric aging processes during transport can further lead to the size-dependent change in the chemical composition of sea salt particles (Dall'Osto et al., 2004; Chi et al., 2015; Bondy et al., 2017). Bondy et al. (2017) found that sulfate was enriched in the submicron sea salt particles while nitrate dominated in the supermicron sea salt particles (Bondy et al., 2017). However, Kirpes et al. (2018) observed that sulfate was also more prevalent than nitrate in supermicron sea salt particles (Kirpes et al., 2018). Additionally, sea salt particles could also react with various organic acids (e.g., oxalate, malonate, and succinate) during transport (Mochida et al., 2003; Laskin et al., 2012). Uncertainty in the formation of secondary species (e.g., sulfate, nitrate, or organic species) would complicate the size-dependent change in the chemical composition of sea salt particles and thus the CCN activity.

Twohy et al. (1989) observed that small ammonium sulfate particles grew to small droplets and large sea salt particles grew to large droplets. Previous observations also considered that the supermicron or giant sea salt-containing particles readily became large cloud droplets, and their CCN behavior was less affected by chemical composition (Noone et al., 1988; Monger et al., 1989; Andreae and Rosenfeld, 2008; Tao et al., 2012). So far, the study on the submicron sea salt-containing particles in cloud droplets is scarce in the literature. Additionally, the existence of secondary species (e.g., sulfate, nitrate, or organic species) onto the submicron sea salt-containing particles might

significantly impact on their cloud activation (O'Dowd et al., 1999; Gibson et al., 2006; Nguyen et al., 2017).

In this study, a ground-based counterflow virtual impactor (GCVI) combined with an online single particle aerosol mass spectrometer (SPAMS) was used to characterize the chemical composition of sea salt-containing cloud residues at Mount Nanling, southern China. This was performed in the downwind direction from the South China Sea during the study period of May-June, 2017. The main goal of this work was to identify the discrepancies in the relative contributions of sea salt-containing particles as a function of the cloud droplet cut size (>7.5 μm, >8.0 μm, >8.5 μm, >9.0 μm, >10.0 μm, >11.0 μm, and >14.0 μm were set in the GCVI system). To elucidate the cloud activity of submicron (dry diameter of 0.2-1.0 μm) sea salt-containing particles, the chemical composition of submicron sea salt-containing particles within various cloud droplet cut sizes was also addressed.

2 Experimental section

2.1 Observation site

The sampling site, which is a National Air Background Monitoring Station, is situated at Mount Nanling, southern China (112°53’56’’ E, 24°41’56’’ N at 1,690 m above sea level). This station is surrounded by a national park forest (273 km^2), minimally affected by local anthropogenic activities. The sampling site is located 50-100 km northeast or north of the Pearl River Delta (PRD) urban agglomeration and 350 km north of the South China Sea (Figure S1). The sampling site is affected by the East

Asian summer monsoon system (Ding and Chan, 2005). Generally, air masses would spend some time traveling across the South China Sea and then travel over the PRD region before reaching the sampling site during the summer period. The SO_2, NOx, NH_3, and volatile organic compound emissions in the PRD region are approximately 711, 891, 195, and 1180 kiloton/yr, respectively (Zheng et al., 2009; Zheng et al., 2012). Hence, the sea salt-containing particles that originate from the South China Sea could interact with anthropogenic gaseous pollutants during their movement across the PRD region.

2.2 Instrumentation

The measurements took place from 18 May-11 June, 2017. The real-time air quality and meteorological parameters were continuously monitored. A GCVI inlet system (GCVI Model 1205, Brechtel Manufacturing Inc.) was used to sample the cloud droplets with various cut sizes. The cloud droplet cut sizes and duration time set in the GCVI system are presented in Table S1. The minimum sampling time for each cut size was 12 hours. The cut size was adjusted by modifying the air velocity in the wind tunnel of the GCVI inlet system (Shingler et al., 2012). It should be noted here that the transmission efficiency increased as the cut size increased (Shingler et al., 2012). The sampled cloud droplets passed through an evaporation chamber to remove the water and the dry residue particles remained. The enrichment factor of the particles that were collected by the GCVI inlet was estimated to range from 6.6 in 7.5 μm to 2.0 in 14.0 μm based on theoretical calculations (Shingler et al., 2012). Pekour and Cziczo (2011)

observed that the breakthrough of large particles tended to increase at the lower size cut. In this study, the number concentration of ambient particles in the GCVI downstream inlet was below 1 cm^3 at the lowest cut sizes during cloud-free periods, hence the large particle breakthrough at the lowest cut size seemed to be quite low. The cloud residues were subsequently characterized using an online SPAMS (Hexin Analytical Instrument Co., Ltd., Guangzhou, China). In order to reliably identify the presence of clouds, an upper-limit visibility of 3 km and a lower-limit relative humidity (RH) of 95% were set in the GCVI software (Lin et al., 2017). During precipitation periods, the GCVI automatically shut down to protect against interference from raindrops.

The SPAMS conducts the real-time characterization the chemical composition of aerosol particles using vacuum aerodynamic diameters (d_{va}) between 0.2 and 2.0 μm. The detailed operations of the SPAMS have been described elsewhere (Li et al., 2011). Briefly, aerosol particles are introduced into the SPAMS through a nozzle inlet. The particle velocity is derived from the measurement of two continuous diode Nd:YAG laser beams (532 nm) and is then converted to the particle size (d_{va}). The particles are subsequently desorbed and ionized by a pulsed laser (266 nm). The positive and negative mass spectra generated are recorded with the corresponding particle size. The laser pulse energy was regulated at 0.5-0.6 mJ during the whole sampling period. Polystyrene latex spheres (Nanosphere Size Standards, Duke Scientific Corp., Palo Alto) of 0.2-2.0 μm in diameter were used to calibrate the sizes of the detected particles. It should be noted that the particles detected by the SPAMS are mostly in the size range

of d_{va} 0.2-2.0 μm (Li et al., 2011).

2.3 Screening of sea salt-containing particles

According to prior laboratory and field studies, sea salt-containing particles generally exhibit a set of sodium-related peaks at m/z 23 $[Na]^+$, 46 $[Na_2]^+$, 62 $[Na_2O]^+$, 63 $[Na_2OH]^+$, 81 $[Na_2{}^{35}Cl]^+$, and 83 $[Na_2{}^{37}Cl]^+$ (Dall'Osto et al., 2004; Herich et al., 2009; Prather et al., 2013). Thus, the sea salt-containing particles in this study were identified by the simultaneous existence of peaks at m/z 23, 46, 62, 63, 81, and 83. Because biologically produced organic species (e.g., m/z -26 $[CN]^-$, -42 $[CNO]^-$, or 59 $[NC_3H_9]^+$) were internally mixed with sodium-related peaks (Prather et al., 2013; Sultana et al., 2017), these primary organic species were not intended to define sea salt-containing particles. Additionally, these organic species might also be produced from secondary aerosol processes (Dall'Osto et al., 2009; Zhang et al., 2012). Therefore, biologically produced organic species that externally mixed with sea salt particles were not considered in the current study. One may expect that chlorine ion peaks at m/z -35 $[^{35}Cl]^-$ or -37 $[^{37}Cl]^-$ in the negative mass spectrum should be considered. Sea salt-containing particles in the atmosphere might not contain chloride due to the complete displacement of chloride by sulfate, nitrate or organic acids during transport (Laskin et al., 2012; Ueda et al., 2014; Arndt et al., 2017). Bondy et al. (2017) also suggested that the identification of sea salt-containing particles without using chloride might give more detailed results on the atmospheric aging processes during transport (Bondy et al., 2017). Thus, a total of 30275 sea salt-containing cloud residues including 8317

submicron and 21958 supermicron particles were obtained in this study.

3 Results and discussion

3.1 General characteristics

Figure 1 displays the hourly averaged data of the meteorological and air quality parameters during the whole sampling period. The wind direction prevailed southwesterly or southerly during the cloud events and most corresponding air masses originated from the South China Sea (Figure S2), which had abundant moist airflows that were probably responsible for the formation of the cloud events. The maximum concentrations of $PM_{2.5}$, SO_2, and NO_X were 76 μg/m^3, 2.8 ppb, and 12 ppb, respectively, during the cloud-free periods. When the cloud events occurred, the levels of $PM_{2.5}$, SO_2, and NO_X clearly decreased, which was indicative of cloud scavenging. The ambient temperature was above 10 ℃ during the whole study period, which allows the formation of liquid cloud droplets.

The average mass spectrum of the sea salt-containing cloud residues during the sampling period is shown in Figure 2. The highest peak at m/z 23 and some small ion peaks at m/z 24 $[Mg]^+$, 39 $[K]^+$, 40 $[Ca]^+$, and 56 $[CaO]^+$ or $[Fe]^+$ were observed in the positive mass spectra. This result was agreement with the previous findings from laboratory and field studies (Guazzotti et al., 2001; Dall'Osto et al., 2004; Gaston et al., 2011; Prather et al., 2013). The significant ion peaks at m/z -46 $[NO_2]^-$ or -62 $[NO_3]^-$ and -97 $[HSO_4]^-$ in the negative mass spectrum represented nitrate and sulfate markers, thus suggesting aged sea salt-containing cloud residues. The presence of organic

197 nitrogen peaks at m/z -26 $[CN]^-$ or -42 $[CNO]^-$ in the negative mass spectrum may be
198 from biologically produced sources or the subsequent accumulation of secondary
199 organic aerosols (Herich et al., 2009; Prather et al., 2013). The small peak areas of other
200 organic species including hydrocarbon organic species (i.e., m/z 15 $[CH_3]^+$, m/z 27
201 $[C_2H_3]^+$ or m/z 43 $[C_2H_3O]^+$), amines (m/z 59 $[C_3H_9N]^+$ or 86 $[C_5H_{12}N]^+$), or organic
202 acids (m/z -89 oxalate, -103 malonate, or -117 succinate) can also be detected in the sea
203 salt-containing cloud residues (Figure S3).
204
205 **3.2 Number fraction and chemical composition of sea salt-containing cloud**
206 **residues**
207 The number fraction (NF) of sea salt-containing particles in the total cloud residues was
208 dependent on the cut sizes. The highest NF was observed at the cut size of 7.5 μm (26%,
209 by number), followed by 14 μm (17%), and the other cut sizes (3-5%) (Figure 3a).
210 These values were higher than the NF (2%, by number) of sea salt-containing particles
211 in the detected ambient aerosol particles during cloud-free periods. Sea salt-containing
212 particles contributed to approximately 1% (by number) of cloud residues at the cut size
213 of 5.0 μm over Mount Schmücke in central Germany, despite air masses that frequently
214 originated over the Atlantic Ocean (Roth et al., 2016). The proportion reached to 5-10%
215 (by number) at the cut size of 11 μm at the North Slope of Alaska (Zelenyuk et al.,
216 2010). Additionally, the cloud water measurement showed that sea salt-containing
217 particles might accumulate in large cloud droplets (Monger et al., 1989). In contrast to
218 these findings, the maximum NF of sea salt-containing cloud residues was found at the

minimum GCVI cut size in this study. Twohy and Anderson (2008) observed an increased NF of sea salt-like cloud residues from coastal areas at the cut size of 20 μm to clean remote oceans at the cut size of 8 μm (Twohy and Anderson, 2008). However, it cannot interpret the enhancement of sea salt-containing cloud residues at the cut size of 7.5 μm in this study because of the comparable air quality and meteorological environments at the all cut sizes.

There was a significant difference in the chemical composition of the sea salt-containing cloud residues between the cut sizes of 7.5 μm and 8-14 μm, as shown in Figure 4. Nitrate was internally mixed with above 90% of the sea salt-containing cloud residues at the all cut sizes. However, notably decreased sulfate (32% versus 87-93%, by number), ammonium (below 1% versus 21-32%), organic nitrogen (70% versus 87-96%), amines (6% versus 30-64%), hydrocarbon organics (2% versus 22-70%), and organic acids (7% versus 42-76%) were found internally mixed with the sea salt-containing cloud residues at the cut size of 7.5 μm compared to 8-14 μm. Roth et al. (2016) found that both sulfate and nitrate were internally mixed with the sea salt-containing cloud residues (Roth et al., 2016). Another study by Zelenyuk et al. (2010) observed that the sea salt-containing cloud residues were composed of four particle types, including fresh NaCl, NaCl internally mixed with nitrate, sulfate and organics. In this study, abundant nitrate was found to internally mix with the sea salt-containing cloud residues at the all cut sizes, while sulfate, ammonium, and organic species showed more diversity between the cut sizes of 7.5 μm and 8-14 μm. These differences in the chemical mixtures of sea salt-containing cloud residues dependent on the location

241 suggest that sea salt-containing particles would experience various ageing process in
242 the atmosphere and subsequently participate in the formation of cloud droplets. More
243 importantly, together with the enrichment of sea salt-containing cloud residues at the
244 minimum cut size of 7.5 μm observed here, this might indicate that the distribution of
245 sea salt-containing cloud residues that were dependent on cloud droplet size is likely
246 influenced by changes in the chemical mixtures of sea salt-containing nuclei. It should
247 be noted here that relative to small cloud droplets, larger cloud droplets might undergo
248 longer duration cloud (Nakajima et al., 2010), thus increase the in-cloud formation of
249 secondary species such as sulfate, ammonium or oxalate. The extreme high fraction of
250 nitrate in the sea salt-containing cloud residues at the all cut sizes was more likely due
251 to the aging processes during atmospheric transport, rather than the in-cloud formation.
252 It is well-known that the chloride depletion in sea salt-containing particles is mainly
253 due to the formation of secondary species, such as sulfate, nitrate, or organic acids
254 (Laskin et al., 2012; Bondy et al., 2017). The chloride depletion might lower the
255 hygroscopic and CCN properties of sea salt-containing particles (i.e., NaCl) (O'Dowd
256 et al., 1999; Gupta et al., 2015). In this study, chloride was internally mixed with above
257 80% (by number) of the sea salt-containing cloud residues at the cut sizes of 8-14 μm,
258 which was clearly higher than 51% at the cut size of 7.5 μm. That is, chloride depletion
259 was weakened in the sea salt-containing cloud residues at the cut sizes of 8-14 μm,
260 despite abundant sulfate and organic acids, as mentioned above. Based on a laboratory
261 study, Ault et al. (2014) found that organic nitrogen can inhibit the heterogeneous
262 reaction of sea salt-containing particles with HNO_3 (Ault et al., 2014). They used a peak

area ratio of chloride to (chloride + nitrate) to estimate the extent of the chloride depletion (Ault et al., 2014). Because the heterogeneous reaction with H_2SO_4, HNO_3, or organic acids and sea salt-containing particles is also present in the atmosphere (Laskin et al., 2012; Chi et al., 2015), a modified peak area ratio (chloride/(chloride + nitrate + sulfate + organic acids)) was applied in the present study. This ratio was found to increase as a function of the increase in the peak area of organic nitrogen, as shown in Figure 5, thereby reflecting the effect of organic nitrogen on the depletion of chloride in sea salt-containing particles in the atmosphere. At the cut sizes of 8-14 μm, abundant organic nitrogen in the sea salt-containing cloud residues likely lowered the chloride depletion. The ratio was not found to be related with the hydrocarbon organic species. The sensitivity of chloride displacement to the presence of organic species was complex (Ault et al., 2014; Bertram et al., 2018), and further studies must be conducted to identify whether diverse organic species affect the heterogeneous reactivity of individual sea salt-containing particles.

3.3 Submicron sea salt-containing cloud residues

The modeling calculation showed that submicron sea salt-containing particles may have a dominant contribution to aerosol-cloud interactions when evaluating the indirect impacts of sea salt aerosols, despite the uncertainty in the sizes and concentrations of sea salt aerosols (Gong, 2003). Few field studies focused on the submicron sea salt-containing particles within cloud droplets. In this work, approximately 25% (by number) of the sea salt-containing cloud residues was found to be at the submicron size. It should

285 be noted that the size distribution of the sea salt-containing cloud residues that were
286 detected by the SPAMS cannot represent the real atmosphere because the highest
287 detection efficiency for the SPAMS was in the size range of 500-800 nm (Li et al., 2011).
288 The relative contribution of sea salt-containing particles to the cloud residues in the
289 given size range is presented to eliminate the detection efficiency of single particle mass
290 spectrometry (Roth et al., 2016), as shown in Figure 3b. At the cut size of 7.5 μm, 20%
291 (by number) of the submicron cloud residues was composed of sea salt-containing
292 particles. This value was prominently higher than that at the cut sizes of 8-14 μm (below
293 2%, by number) or that during cloud-free periods (1%) (Figure S4). The difference at
294 least reflects that the submicron sea salt-containing particles could be enriched in the
295 small cloud droplets.

296 The diverse chemical composition of the submicron sea salt-containing cloud
297 residues was found between the cut sizes of 7.5 μm and 8-14 μm. At the cut size of 7.5
298 μm, nitrate was internally mixed with 90% (by number) of the submicron sea salt-
299 containing cloud residues, which was much higher than the fractions of sulfate (20%)
300 and ammonium (below 1%) (Figure 4). It implies that the secondary inorganic species
301 in the submicron sea salt-containing cloud residues at the cut size of 7.5 μm was
302 dominated by nitrate, mostly from the partitioning and heterogeneous/aqueous
303 chemistry of HNO_3 and other precursors (e.g., N_2O_5) in the atmosphere (Chang et al.,
304 2011; Schneider et al., 2017). However, prominently higher fractions of sulfate (86-
305 94%, by number) and ammonium (38-83%) were found to internally mix with the
306 submicron sea salt-containing cloud residues at the cut sizes of 8-14 μm, thus reflecting

more chemically aged or longer cloud processes. This was also supported by the increase of the relative peak areas of these secondary species in the submicron sea salt-containing cloud residues at the cut sizes of 8-14 μm compared to 7.5 μm (Figure S5). The enrichment of sulfate in the submicron sea salt-containing particles has also extensively been reported in the literature (Jourdain et al., 2008; Kelly et al., 2010; Bondy et al., 2017), which is largely a result of the preferential formation of sulfate in submicron particle sizes with great surface area-to-volume ratios (Song and Carmichael, 1999). Initially, fresh sea salt-containing particles generally appear to be alkaline due to carbonate, and they subsequently experience the reactive uptake of SO_2, H_2SO_4, or HNO_3 during transport (Sievering et al., 1999; Alexander et al., 2005). The lack of ammonium suggests that the accumulated secondary acids during transport insufficiently acidize the submicron sea salt-containing cloud residues at the cut size of 7.5 μm, which, in turn, causes the uptake of gaseous NH_3 to fail. In contrast, the accumulated ammonium in the submicron sea salt-containing cloud residues at the cut sizes of 8-14 μm (Figure 4) indicate that the alkaline sea salt-containing cloud residues have been eventually consumed by secondary acids and thus uptake gaseous NH_3 to neutralize these acidic species (Song and Carmichael, 1999). Furthermore, higher number fraction of amines was found to internally mix with the submicron sea salt-containing cloud residues at the cut sizes of 8-14 μm compared to 7.5 μm (71-87% versus 6%, by number). Despite the biologically produced amines being internally mixed with fresh sea salt-containing particles (Sultana et al., 2017), a similar feature of ammonium and amines in the submicron sea salt-containing cloud residues observed

here implies that the presence of amines mainly comes from the partitioning of the gas into the aqueous phase, particularly during cloud processing (Roth et al., 2016; Lin et al., 2017).

A laboratory study showed that biologically produced organic nitrogen that internally mixed with freshly sea salt-containing particles was found to increase in the submicron size range (Prather et al., 2013). This likely led to the enrichment of organic nitrogen (58%, by number) relative to hydrocarbon organic species (2%) or organic acids (4%) in the submicron sea salt-containing cloud residues at the cut size of 7.5 μm (Figure 4). Meanwhile, at the cut sizes of 8-14 μm, higher fractions of organic nitrogen (80-94%, by number), hydrocarbon organic species (52-90%), and organic acids (32-77%) were observed (Figure 4), indicative of the more chemically aged processes, as mentioned above. Note that magnesium and calcium internally mixed with above 85% (by number) and above 88% of the submicron sea salt-containing cloud residues at the cut sizes of 8-14 μm might increase the presence of organic nitrogen due to the probable complexation with organic species and these cations (Bertram et al., 2018). Hydrocarbon organic particle types coupled with the peak area Mg >> Na can be produced from biological sources in seawater, but they are externally mixed with fresh submicron sea salt-containing particles (Sultana et al., 2017). Thus, the abundant hydrocarbon organics observed here might originate from accumulation during transport. The uptake of gaseous organic acids or the organic acids that formed through heterogeneous reactions were responsible for the increased organic acids presented herein (Mochida et al., 2003; Sullivan and Prather, 2007). We cannot preclude that the

decreased organic species of the submicron sea salt-containing particles at the cut size of 7.5 μm might be also due to having shorter duration cloud relative to other cut sizes. Further study needs to compare the contribution of aging degree during transport and duration time of cloud process to the secondary species.

Petters and Kreidenweis (2007) described the CCN activity of multicomponent aerosol particles using a single parameter (κ) as follows: $\kappa = \varepsilon_{org} * \kappa_{org} + \varepsilon_{inorg} * \kappa_{inorg}$; where ε_{org} and ε_{inorg} represent the bulk volume fractions of organic and inorganic species, respectively, and κ_{org} (generally below 0.5 for organic species) and κ_{inorg} (1.28 for NaCl, 0.88 for $NaNO_3$, 0.80 for Na_2SO_4, 0.67 for NH_4NO_3, and 0.61 for $(NH_4)_2SO_4$) refer to the CCN-derived hygroscopicity parameters of the organic and inorganic species, respectively. Relative to the cut sizes of 8-14 μm, the reduction of organic species in the submicron sea salt-containing cloud residues at the cut size of 7.5 μm is likely to increase κ and hence CCN property. Additionally, the submicron sea salt particles contained higher proportions of organic nitrogen (73-94% versus 58%, by number), hydrocarbon organic species (51-81% versus 2%) and organic acids (35-72% versus 4%) in the ambient aerosol particles than in the cloud residues at cut size of 7.5 μm. This further supports that the enhancement of organic species in the submicron particles likely reduced CCN activity of sea salt particles.

3.4 Supermicron sea salt-containing cloud residues

The supermicron (dry diameter of 1.0-2.0 μm) sea salt-containing particles contributed more to cloud residues with the increasing cut sizes (Figure 3b). For instance, up to 70%

of the supermicron cloud residues were found to consist of sea salt-containing particles at the maximum cut size of 14 μm. The enrichment of the large supermicron or giant sea salt-containing particles in large cloud droplets has also been reported in previous studies (Noone et al., 1988; Twohy et al., 1989; Tao et al., 2012). Nitrate was internally mixed with above 90% (by number) of the supermicron sea salt-containing cloud residues at the all cut sizes (Figure 4). The proportions of sulfate, ammonium, and organic species in supermicron sea salt-containing cloud residues at the cut size of 7.5 μm were lower than those at the cut sizes of 8-14 μm (Figure 4), which was similar to the submicron particles. However, the increased organic species in the supermicron sea salt-containing cloud residues at the cut sizes of 8-14 μm was not expected to reduce their CCN behavior. It was likely that their CCN activity was less affected by the change in the chemical composition. For coarse or giant nuclei (dry particle size > 1 μm), their CCN abilities were dependent on their size rather than their chemical composition (Andreae and Rosenfeld, 2008; Tao et al., 2012). Hudson and Rogers (1986) also found that large nuclei increased in large cloud droplets due to lower critical supersaturation of larger nuclei compared to smaller nuclei (Hudson and Rogers, 1986).

4 Atmospheric implications and conclusion

This work focused on the size-resolved chemical composition of sea salt-containing cloud residues as a function of the cloud droplet cut size. Nitrate internally mixed with above 95% (by number) of the sea salt-containing cloud residues at the all cut sizes emphasized that the sea salt-containing nuclei had undergone chemical evolution

during transport. For simplicity, modeling simulations assumed that the externally mixed NaCl and secondary species (e.g., sulfate) mode or pure NaCl instead of sea salt aerosols was used to predict the size-dependent cloud droplets chemistry or the residence time of sea salt aerosols in the atmosphere (Twohy et al., 1989; Gong et al., 2002; Ma et al., 2008). The change of chemical composition of the submicron sea salt-containing particles might have an impact on their CCN activity. Our result showed that the reduction of organic species in the submicron sea salt-containing cloud residues at the cut size of 7.5 μm is likely to increase CCN activity, leading to the enrichment of the submicron sea salt-containing particles. The resulting effect might prolong the residence time of submicron sea salt-containing aerosols in the atmosphere. This differed from the supermicron sea salt-containing particles, which readily become large cloud droplets, consistent with the previous measurements (Noone et al., 1988; Yuan et al., 2008). More work is needed to evaluate the contribution of atmospheric aged processes to the change of the chemical composition that is associated with the CCN activity of sea salt-containing particles, particularly in the submicron size range.

Data availability.

All the data can be obtained by contacting the corresponding author Xinhui Bi (bixh@gig.ac.cn).

Author contribution.

XHB, GHZ, and QHL planned and designed the experimental setup. YXY, YZF, LP, FJ,

XFL, FXL, and JO performed the atmospheric measurement and collected the data. QHL and XHB analyzed the data and wrote the manuscript. LL, DHC, ML, MJT, XMW, PAP, and GYS contributed comments.

Acknowledgements.

This work was supported by the National Key Research and Development Program of China (2017YFC0210104), the National Nature Science Foundation of China (No. 41877307, 41775124 and 41805103), the Foundation for Leading Talents of the Guangdong Province Government, and the State Key Laboratory of Organic Geochemistry (SKLOG2016-A05). The authors also acknowledge the NOAA Air Resources Laboratory for the provision of the HYSPLIT transport and dispersion model and READY website (http://ready.arl.noaa.gov) used in this publication.

Competing interests.

The authors declare that they have no conflict of interest.

References

Alexander, B., Park, R. J., Jacob, D. J., Li, Q. B., Yantosca, R. M., Savarino, J., Lee, C. C. W., and Thiemens, M. H.: Sulfate formation in sea-salt aerosols: Constraints from oxygen isotopes, J. Geophys. Res.-Atmos., 110, D10307, https://doi.org/10.1029/2004jd005659, 2005.

Andreae, M. O., and Rosenfeld, D.: Aerosol-cloud-precipitation interactions. Part 1. The nature and sources of cloud-active aerosols, Earth-Sci. Rev., 89, 13-41,

https://doi.org/10.1016/j.earscirev.2008.03.001, 2008.

Arndt, J., Sciare, J., Mallet, M., Roberts, G. C., Marchand, N., Sartelet, K., Sellegri, K., Dulac, F., Healy, R. M., and Wenger, J. C.: Sources and mixing state of summertime background aerosol in the north-western Mediterranean basin, Atmos. Chem. Phys., 17, 6975-7001, https://doi.org/10.5194/acp-17-6975-2017, 2017.

Ault, A. P., Guasco, T. L., Baltrusaitis, J., Ryder, O. S., Trueblood, J. V., Collins, D. B., Ruppel, M. J., Cuadra-Rodriguez, L. A., Prather, K. A., and Grassian, V. H.: Heterogeneous reactivity of nitric acid with nascent sea spray aerosol: Large differences observed between and within individual particles, J. Phys. Chem. Lett., 5, 2493-2500, https://doi.org/10.1021/jz5008802, 2014.

Bertram, T. H., Cochran, R. E., Grassian, V. H., and Stone, E. A.: Sea spray aerosol chemical composition: Elemental and molecular mimics for laboratory studies of heterogeneous and multiphase reactions, Chem. Soc. Rev., 47, 2374-2400, https://doi.org/10.1039/C7CS00008A, 2018.

Bondy, A. L., Wang, B., Laskin, A., Craig, R. L., Nhliziyo, M. V., Bertman, S. B., Pratt, K. A., Shepson, P. B., and Ault, A. P.: Inland sea spray aerosol transport and incomplete chloride depletion: Varying degrees of reactive processing observed during SOAS, Environ. Sci. Technol., 51, 9533-9542, https://doi.org/10.1021/acs.est.7b02085, 2017.

Boucher, O., Randall, D., Artaxo, P., Bretherton, C., Feingold, G., Forster, P., Kerminen, V., Kondo, Y., Liao, H., Lohmann, U., Rasch, P., Satheesh, S., Sherwood, S., Stevens, B., and Zhang, X.: Clouds and Aerosols, in: Climate Change 2013: The

Physical Science Basis. Contribution of Working Group I to the Fifth Assessment Report of the Intergovernmental Panel on Climate Change, edited by: Stocker, T. F., Qin, D., Plattner, G.K., Tignor, M., Allen, S. K., Boschung, J., Nauels, A., Xia, Y., Bex, V., and Midgley, P. M., Cambridge University Press, Cambridge, UK and New York, NY, USA, 571-657, 2013.

Chang, W. L., Bhave, P. V., Brown, S. S., Riemer, N., Stutz, J., and Dabdub, D.: Heterogeneous atmospheric chemistry, ambient measurements, and model calculations of N_2O_5: A review, Aerosol Sci. Tech., 45, 665-695, https://doi.org/10.1080/02786826.2010.551672, 2011.

Chi, J. W., Li, W. J., Zhang, D. Z., Zhang, J. C., Lin, Y. T., Shen, X. J., Sun, J. Y., Chen, J. M., Zhang, X. Y., Zhang, Y. M., and Wang, W. X.: Sea salt aerosols as a reactive surface for inorganic and organic acidic gases in the Arctic troposphere, Atmos. Chem. Phys., 15, 11341-11353, https://doi.org/10.5194/acp-15-11341-2015, 2015.

Cochran, R. E., Ryder, O. S., Grassian, V. H., and Prather, K. A.: Sea spray aerosol: The chemical link between the oceans, atmosphere, and climate, Accounts Chem. Res., 50, 599-604, https://doi.org/10.1021/acs.accounts.6b00603, 2017.

Dadashazar, H., Wang, Z., Crosbie, E., Brunke, M., Zeng, X. B., Jonsson, H., Woods, R. K., Flagan, R. C., Seinfeld, J. H., and Sorooshian, A.: Relationships between giant sea salt particles and clouds inferred from aircraft physicochemical data, J. Geophys. Res.-Atmos., 122, 3421-3434, https://doi.org/10.1002/2016JD026019, 2017.

Dall'Osto, M., Beddows, D. C. S., Kinnersley, R. P., Harrison, R. M., Donovan, R. J.,

and Heal, M. R.: Characterization of individual airborne particles by using aerosol time-of-flight mass spectrometry at Mace Head, Ireland, J. Geophys. Res.-Atmos., 109, D21302, https://doi.org/10.1029/2004jd004747, 2004.

Dall'Osto, M., Harrison, R., Coe, H., and Williams, P.: Real-time secondary aerosol formation during a fog event in London, Atmos. Chem. Phys., 9, 2459-2469, https://doi.org/10.5194/acp-9-2459-2009, 2009.

Ding, Y., and Chan, J. C. L.: The East Asian summer monsoon: An overview, Meteorol. Atmos. Phys., 89, 117-142, https://doi.org/10.1007/s00703-005-0125-z, 2005.

Gantt, B., and Meskhidze, N.: The physical and chemical characteristics of marine primary organic aerosol: A review, Atmos. Chem. Phys., 13, 3979-3996, https://doi.org/10.5194/acp-13-3979-2013, 2013.

Gaston, C. J., Furutani, H., Guazzotti, S. A., Coffee, K. R., Bates, T. S., Quinn, P. K., Aluwihare, L. I., Mitchell, B. G., and Prather, K. A.: Unique ocean-derived particles serve as a proxy for changes in ocean chemistry, J. Geophys. Res.-Atmos., 116, D18310, https://doi.org/10.1029/2010JD015289, 2011.

Gibson, E. R., Hudson, P. K., and Grassian, V. H.: Physicochemical properties of nitrate aerosols: Implications for the atmosphere, J. Phys. Chem. A, 110, 11785-11799, https://doi.org/10.1021/jp063821k, 2006.

Gong, S. L., Barrie, L. A., and Lazare, M.: Canadian Aerosol Module (CAM): A size-segregated simulation of atmospheric aerosol processes for climate and air quality models 2. Global sea-salt aerosol and its budgets, J. Geophys. Res.-Atmos., 107, D24, 4779, https://doi.org/10.1029/2001jd002004, 2002.

505 Gong, S. L.: A parameterization of sea-salt aerosol source function for sub- and super-
506 micron particles, Global Biogeochem. Cycles, 17, 1097,
507 https://doi.org/10.1029/2003gb002079, 2003.
508 Guazzotti, S. A., Coffee, K. R., and Prather, K. A.: Continuous measurements of size-
509 resolved particle chemistry during INDOEX-intensive field phase 99, J. Geophys.
510 Res.-Atmos., 106, 28607-28627, https://doi.org/10.1029/2001jd900099, 2001.
511 Gupta, D., Kim, H., Park, G., Li, X., Eom, H. J., and Ro, C. U.: Hygroscopic properties
512 of NaCl and $NaNO_3$ mixture particles as reacted inorganic sea-salt aerosol
513 surrogates, Atmos. Chem. Phys., 15, 3379-3393, https://doi.org/10.5194/acp-15-
514 3379-2015, 2015.
515 Herich, H., Kammermann, L., Friedman, B., Gross, D. S., Weingartner, E., Lohmann,
516 U., Spichtinger, P., Gysel, M., Baltensperger, U., and Cziczo, D. J.: Subarctic
517 atmospheric aerosol composition: 2. Hygroscopic growth properties, J. Geophys.
518 Res.-Atmos., 114, D13204, https://doi.org/10.1029/2008jd011574, 2009.
519 Hudson, J. G., and Rogers, C. F.: Relationship between critical supersaturation and
520 cloud droplets size-implications for cloud mixing processes, J. Atmos. Sci., 43,
521 2341-2359, https://doi.org/10.1175/1520-0469(1986)043<2341:Rbcsac>2.0.Co;2,
522 1986.
523 Jourdain, B., Preunkert, S., Cerri, O., Castebrunet, H., Udisti, R., and Legrand, M.:
524 Year-round record of size-segregated aerosol composition in central Antarctica
525 (Concordia station): Implications for the degree of fractionation of sea-salt
526 particles, J. Geophys. Res.-Atmos., 113, D14308,

https://doi.org/10.1029/2007jd009584, 2008.

Kelly, J., Bhave, P., Nolte, C., Shankar, U., and Foley, K.: Simulating emission and chemical evolution of coarse sea-salt particles in the Community Multiscale Air Quality (CMAQ) model, Geosci. Model Dev., 3, 257-273, https://doi.org/10.5194/gmd-3-257-2010, 2010.

Kirpes, R. M., Bondy, A. L., Bonanno, D., Moffet, R. C., Wang, B., Laskin, A., Ault, A. P., and Pratt, K. A.: Secondary sulfate is internally mixed with sea spray aerosol and organic aerosol in the winter Arctic, Atmos. Chem. Phys., 18, 3937-3949, https://doi.org/10.5194/acp-18-3937-2018, 2018.

Laskin, A., Moffet, R. C., Gilles, M. K., Fast, J. D., Zaveri, R. A., Wang, B., Nigge, P., and Shutthanandan, J.: Tropospheric chemistry of internally mixed sea salt and organic particles: Surprising reactivity of NaCl with weak organic acids, J. Geophys. Res.-Atmos., 117, D15302, https://doi.org/10.1029/2012jd017743, 2012.

Li, L., Huang, Z., Dong, J., Li, M., Gao, W., Nian, H., Fu, Z., Zhang, G., Bi, X., Cheng, P., and Zhou, Z.: Real time bipolar time-of-flight mass spectrometer for analyzing single aerosol particles, Int. J. Mass Spectrom., 303, 118-124, https://doi.org/10.1016/j.ijms.2011.01.017, 2011.

Lin, Q., Zhang, G., Peng, L., Bi, X., Wang, X., Brechtel, F. J., Li, M., Chen, D., Peng, P., amp, apos, an, Sheng, G., and Zhou, Z.: In situ chemical composition measurement of individual cloud residue particles at a mountain site, southern China, Atmos. Chem. Phys., 17, 8473-8488, https://doi.org/10.5194/acp-17-8473-

549 2017, 2017.
550 Ma, X., Von Salzen, K., and Li, J.: Modelling sea salt aerosol and its direct and indirect
551 effects on climate, Atmos. Chem. Phys., 8, 1311-1327,
552 https://doi.org/10.5194/acp-8-1311-2008, 2008.
553 Mochida, M., Umemoto, N., Kawamura, K., and Uematsu, M.: Bimodal size
554 distribution of C_2–C_4 dicarboxylic acids in the marine aerosols, Geophys. Res.
555 Lett., 30, 1672, https://doi.org/10.1029/2003GL017451, 2003.
556 Monger, J. W., Jr, J. C., Jr, B. D., and Hoffmann, M. R.: Chemical composition of
557 coastal stratus clouds: Dependence on droplet size and distance from the coast,
558 Atmos. Environ., 23, 2305-2320, https://doi.org/10.1016/0004-6981(89)90192-3,
559 1989.
560 Nakajima, T. Y., Suzuki, K., and Stephens, G. L., Droplet growth in warm water clouds
561 observed by the A-Train. Part II: A multisensor view. J. Atmos. Sci., 67, 1897-
562 1907, https://doi.org/10.1175/2010JAS3276.1, 2010.
563 Nguyen, Q.T., Kjaer, K.H., Kling, K.I., Boesen, T., and Bilde, M.: Impact of fatty acid
564 coating on the CCN activity of sea salt particles, Tellus B, 69, 1304064,
565 https://doi.org/10.1080/16000889.2017.1304064, 2017.
566 Noone, K. J., Charlson, R. J., Covert, D. S., Ogren, J. A., and Heintzenberg, J.: Cloud
567 droplets: Solute concentration is size dependent, J. Geophys. Res.-Atmos., 93,
568 9477-9482, https://doi.org/10.1029/JD093iD08p09477, 1988.
569 O'Dowd, C. D., Lowe, J. A., and Smith, M. H.: Coupling sea-salt and sulphate
570 interactions and its impact on cloud droplets concentration predictions, Geophys.

571 Res. Lett., 26, 1311-1314, https://doi.org/10.1029/1999gl900231, 1999.
572 Petters, M. D., and Kreidenweis, S. M.: A single parameter representation of
573 hygroscopic growth and cloud condensation nucleus activity, Atmos. Chem. Phys.,
574 7, 1961-1971, https://doi.org/10.5194/acp-7-1961-2007, 2007.
575 Pierce, J. R., and Adams, P. J.: Global evaluation of CCN formation by direct emission
576 of sea salt and growth of ultrafine sea salt, J. Geophys. Res.-Atmos., 111, D06203,
577 https://doi.org/10.1029/2005jd006186, 2006.
578 Prather, K. A., Bertram, T. H., Grassian, V. H., Deane, G. B., Stokes, M. D., Demott, P.
579 J., Aluwihare, L. I., Palenik, B. P., Azam, F., and Seinfeld, J. H.: Bringing the
580 ocean into the laboratory to probe the chemical complexity of sea spray aerosol, P.
581 Natl. Acad. Sci. USA, 110, 7550-7555, https://doi.org/10.1073/pnas.1300262110,
582 2013.
583 Quinn, P. K., Collins, D. B., Grassian, V. H., Prather, K. A., and Bates, T. S.: Chemistry
584 and related properties of freshly emitted sea spray aerosol, Chem. Rev., 115, 4383-
585 4399, https://doi.org/10.1021/cr500713g, 2015.
586 Roth, A., Schneider, J., Klimach, T., Mertes, S., van Pinxteren, D., Herrmann, H., and
587 Borrmann, S.: Aerosol properties, source identification, and cloud processing in
588 orographic clouds measured by single particle mass spectrometry on a central
589 European mountain site during HCCT-2010, Atmos. Chem. Phys., 16, 505-524,
590 https://doi.org/10.5194/acp-16-505-2016, 2016.
591 Schneider, J., Mertes, S., van Pinxteren, D., Herrmann, H., and Borrmann, S.: Uptake
592 of nitric acid, ammonia, and organics in orographic clouds: mass spectrometric

593 analyses of droplet residual and interstitial aerosol particles, Atmos. Chem. Phys.,
594 17, 1571-1593, https://doi.org/10.5194/acp-17-1571-2017, 2017.
595 Shingler, T., Dey, S., Sorooshian, A., Brechtel, F. J., Wang, Z., Metcalf, A., Coggon, M.,
596 Mülmenstädt, J., Russell, L. M., Jonsson, H. H., and Seinfeld, J. H.:
597 Characterisation and airborne deployment of a new counterflow virtual impactor
598 inlet, Atmos. Meas. Tech., 5, 1259-1269, https://doi.org/10.5194/amt-5-1259-
599 2012, 2012.
600 Sievering, H., Lerner, B., Slavich, J., Anderson, J., Pósfai, M., and Cainey, J.: O_3
601 oxidation of SO_2 in sea-salt aerosol water: Size distribution of non-sea-salt sulfate
602 during the First Aerosol Characterization Experiment (ACE 1), J. Geophys. Res.-
603 Atmos., 104, 21707-21717, https://doi.org/10.1029/1998jd100086, 1999.
604 Song, C. H., and Carmichael, G. R.: The aging process of naturally emitted aerosol
605 (sea-salt and mineral aerosol) during long range transport, Atmos. Environ., 33,
606 2203-2218, https://doi.org/10.1016/S1352-2310(98)00301-X, 1999.
607 Sullivan, R. C., and Prather, K. A.: Investigations of the diurnal cycle and mixing state
608 of oxalic acid in individual particles in Asian aerosol outflow, Environ. Sci.
609 Technol., 41, 8062-8069, https://doi.org/10.1021/es071134g. 2007.
610 Sultana, C. M., Collins, D. B., and Prather, K. A.: Effect of structural heterogeneity in
611 chemical composition on online single-particle mass spectrometry analysis of sea
612 spray aerosol particles, Environ. Sci. Technol., 51, 3660-3668,
613 https://doi.org/10.1021/acs.est.6b06399, 2017.
614 Tao, W. K., Chen, J. P., Li, Z. Q., Wang, C., and Zhang, C. D.: Impact of aerosols on

615 convective clouds and precipitation, Rev. Geophys., 50, RG2001,
616 https://doi.org/10.1029/2011rg000369, 2012.
617 Twohy, C. H., Austin, P. H., and Charlson, R. J.: Chemical consequences of the initial
618 diffusional growth of cloud droplets: A clean marine case, Tellus B, 41, 51-60,
619 https://doi.org/10.1111/j.1600-0889.1989.tb00124.x, 1989.
620 Twohy, C. H., and Anderson, J. R.: Droplet nuclei in non-precipitating clouds:
621 Composition and size matter, Environ. Res. Lett., 3, 045002,
622 https://doi.org/10.1088/1748-9326/3/4/045002, 2008.
623 Ueda, S., Hirose, Y., Miura, K., and Okochi, H.: Individual aerosol particles in and
624 below clouds along a Mt. Fuji slope: Modification of sea-salt-containing particles
625 by in-cloud processing, Atmos. Res., 137, 216-227,
626 https://doi.org/10.1016/j.atmosres.2013.10.011, 2014.
627 Wang, X., Sultana, C. M., Trueblood, J., Hill, T. C., Malfatti, F., Lee, C., Laskina, O.,
628 Moore, K. A., Beall, C. M., McCluskey, C. S., Cornwell, G. C., Zhou, Y., Cox, J.
629 L., Pendergraft, M. A., Santander, M. V., Bertram, T. H., Cappa, C. D., Azam, F.,
630 DeMott, P. J., Grassian, V. H., and Prather, K. A.: Microbial control of sea spray
631 aerosol composition: A tale of two blooms, ACS Central Sci., 1, 124-131,
632 https://doi.org/10.1021/acscentsci.5b00148, 2015.
633 Yuan, T., Li, Z., Zhang, R., and Fan, J.: Increase of cloud droplets size with aerosol
634 optical depth: An observation and modeling study, J. Geophys. Res.-Atmos., 113,
635 D04201, https://doi.org/10.1029/2007jd008632, 2008.
636 Zelenyuk, A., Imre, D., Earle, M., Easter, R., Korolev, A., Leaitch, R., Liu, P.,

637 Macdonald, A. M., Ovchinnikov, M., and Strapp, W.: In situ characterization of
638 cloud condensation nuclei, interstitial, and background particles using the single
639 particle mass spectrometer, SPLAT II†, Anal. Chem., 82, 7943-7951,
640 https://doi.org/10.1021/ac1013892, 2010.
641 Zhang, G., Bi, X., Chan, L. Y., Li, L., Wang, X., Feng, J., Sheng, G., Fu, J., Li, M., and
642 Zhou, Z.: Enhanced trimethylamine-containing particles during fog events
643 detected by single particle aerosol mass spectrometry in urban Guangzhou, China,
644 Atmos. Environ., 55, 121-126, https://doi.org/10.1016/j.atmosenv.2012.03.038,
645 2012.
646 Zheng, J., Zhang, L., Che, W., Zheng, Z., and Yin, S.: A highly resolved temporal and
647 spatial air pollutant emission inventory for the Pearl River Delta region, China and
648 its uncertainty assessment, Atmos. Environ., 43, 5112-5122,
649 https://doi.org/10.1016/j.atmosenv.2009.04.060, 2009.
650 Zheng, J., Yin, S. S., Kang, D. W., Che, W. W., and Zhong, L. J.: Development and
651 uncertainty analysis of a high-resolution NH_3 emissions inventory and its
652 implications with precipitation over the Pearl River Delta region, China, Atmos.
653 Chem. Phys., 12, 7041-7058, https://doi.org/10.5194/acp-12-7041-2012, 2012.

Figure captions:

Figure 1. The hourly averaged data of meteorological and air quality parameters.

Figure 2. The averaged mass spectrum of the sea salt-containing cloud residues.

Figure 3. Number fraction or counts of sea salt-containing cloud residues as a function of the cut size (a) and the relative contribution of sea salt-containing cloud residues to the total cloud residues in the given size range (b).

Figure 4. Mixed fractions of inorganic and organic species in the sea salt-containing cloud residues. The mixing fraction is defined as the number particles of a given compound divided by the total number particles. The inorganic species include sulfate (m/z -97), nitrate (m/z -46 or -62), chloride (m/z -35 or -37), ammonium (m/z 18), magnesium (m/z 24), and calcium (m/z 40). The organic species include organic nitrogen (m/z -26 or -42), amines (m/z 59 or 86), CH_3 (m/z 15), C_2H_3 (m/z 27), C_2H_3O (m/z 43), oxalate (m/z -89), malonate (m/z -103), and succinate (m/z -117).

Figure 5. Ratios as a function of the organic nitrogen (m/z -26 or -42) peak area. The ratios refer to the chloride (m/z -35 or -37) peak area divided by the sum of the sulfate (m/z -97), nitrate (m/z -46 or -62), organic acids (m/z -89, -103, or -117), and chloride peak areas, as explained in the text.

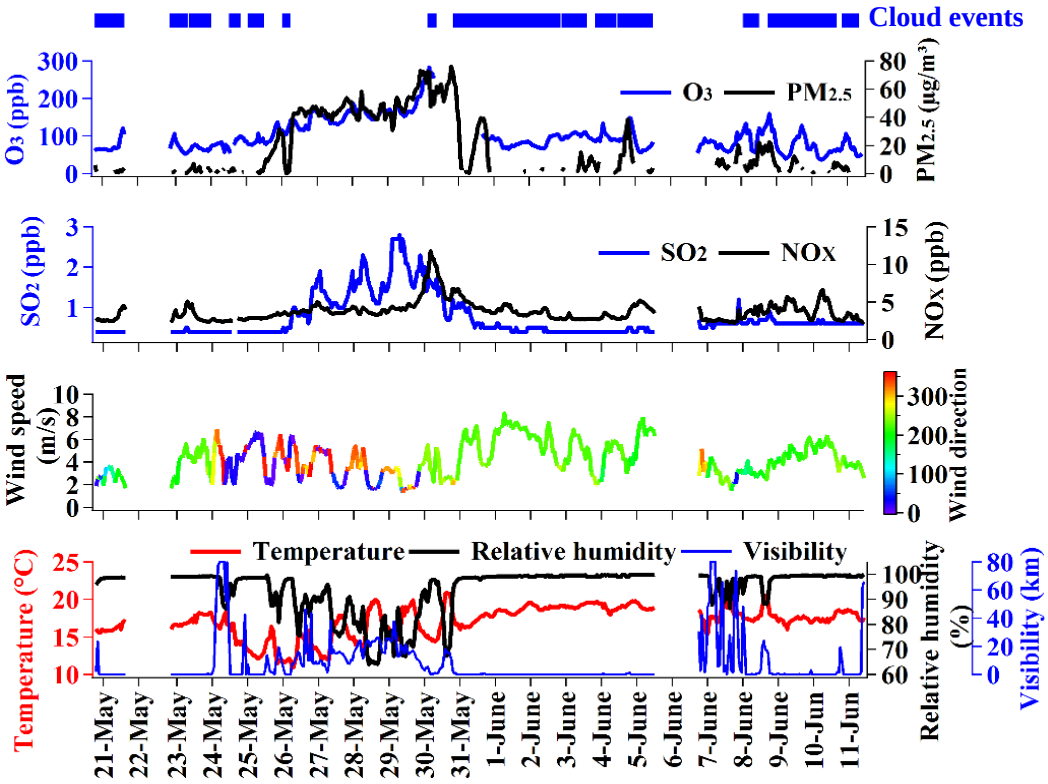
Cloud events
O3 (ppb)
PM2.5 (μg/m³)
O3
PM2.5
SO2 (ppb)
NOX (ppb)
SO2
NOX
Wind speed (m/s)
Wind direction
Temperature (°C)
Relative humidity (%)
Visibility (km)
Temperature
Relative humidity
Visibility
21-May
22-May
23-May
24-May
25-May
26-May
27-May
28-May
29-May
30-May
31-May
1-June
2-June
3-June
4-June
5-June
6-June
7-June
8-June
9-June
10-Jun
11-Jun

672 Figure 1

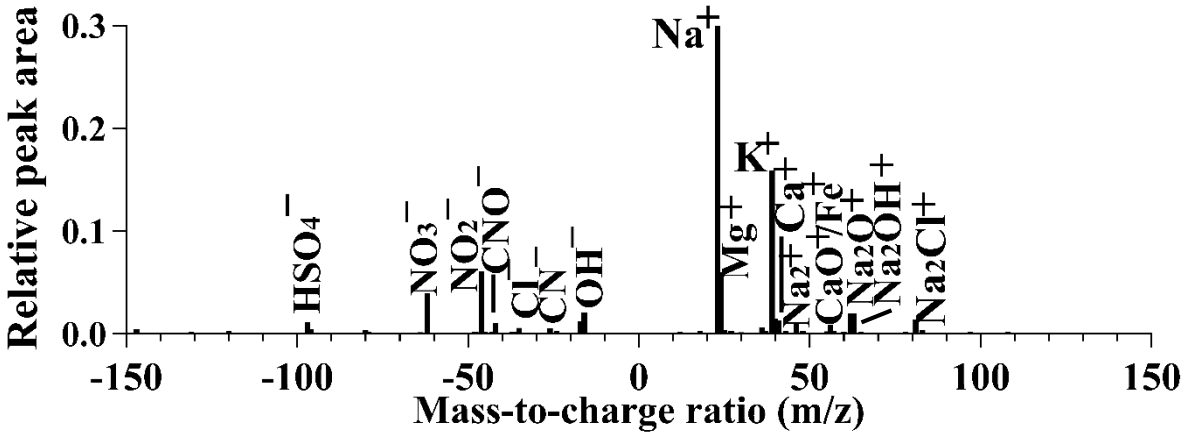

673

674 Figure 2

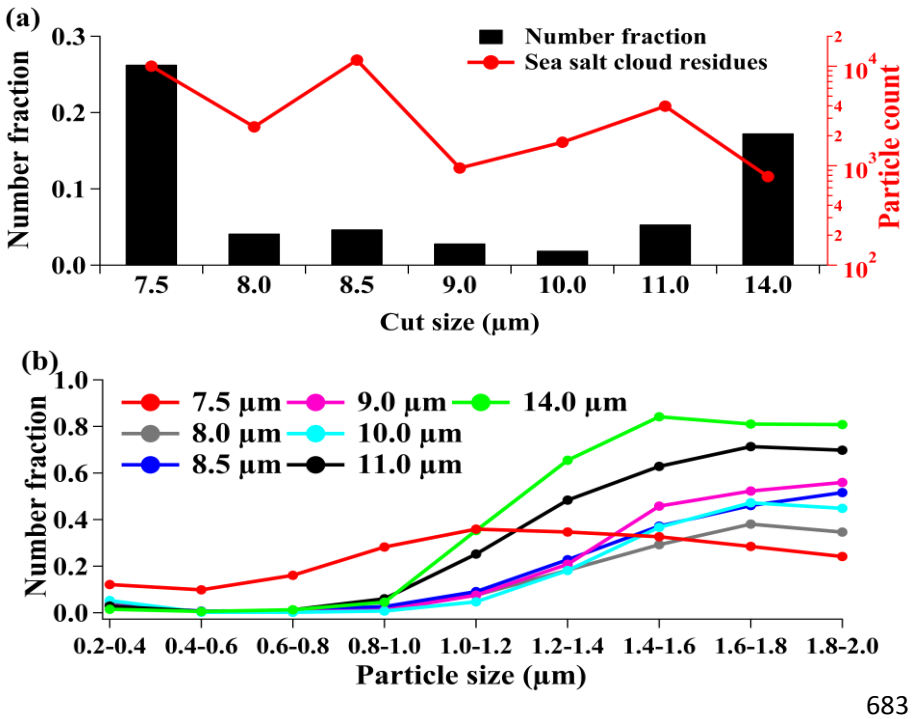

683

684 Figure 3

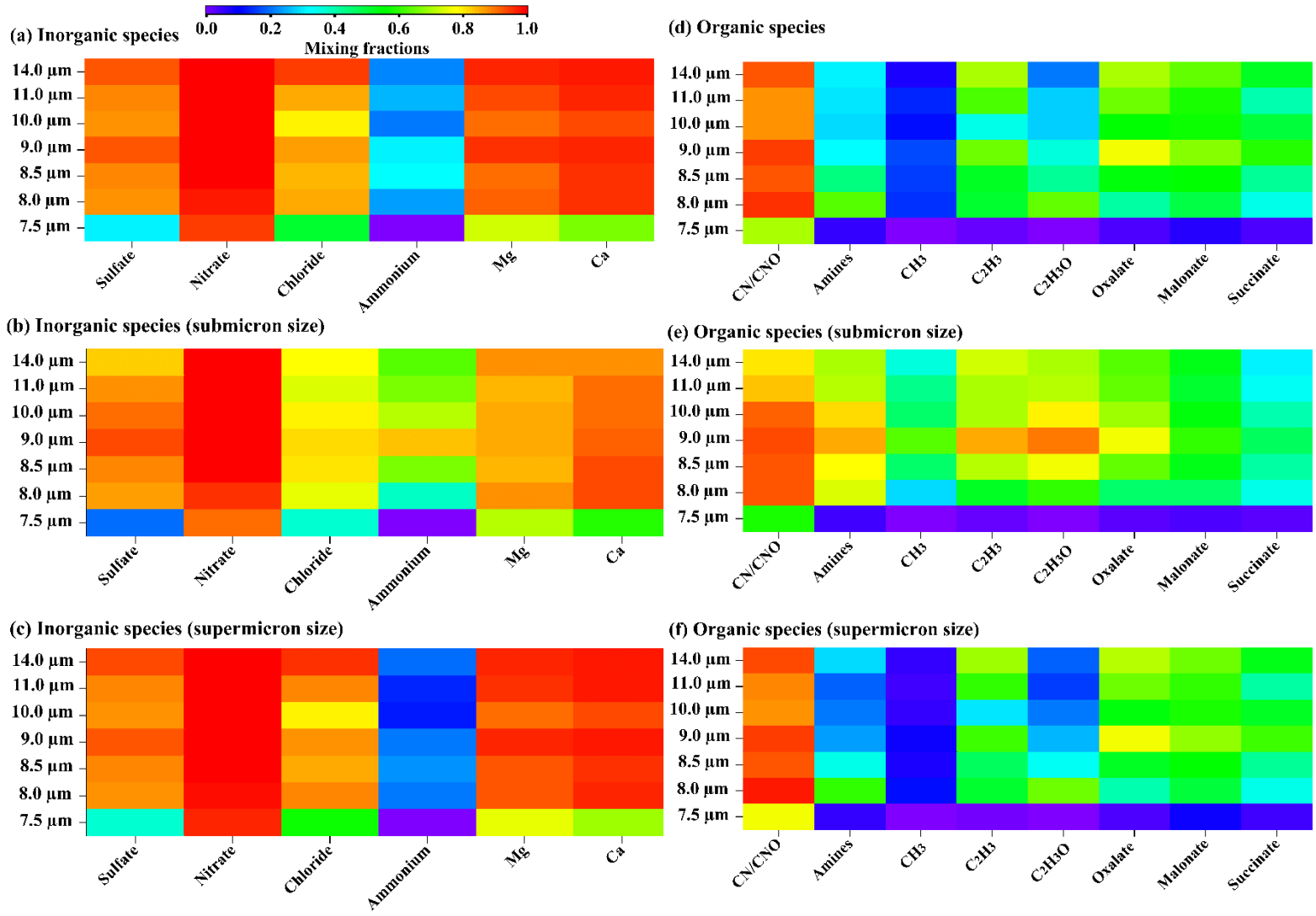

685

686 Figure 4

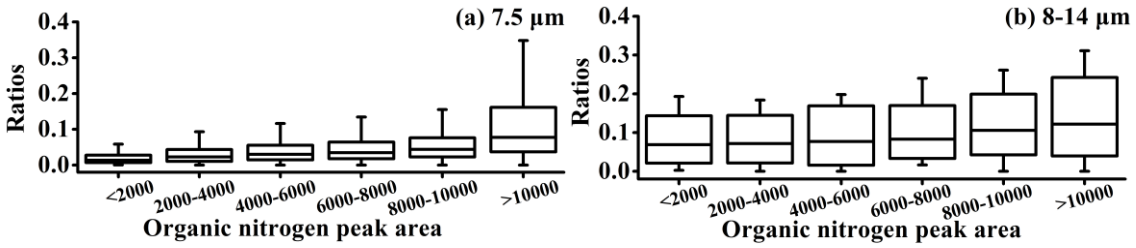

687

688 Figure 5

689

690